THE JOURNAL OF PHYSICAL CHEMISTRY B

Article

pubs.acs.org/JPCB

Unveiling the Eigen-Weller Ion Pair from the Excited State Proton Transfer Kinetics of 3-Chloro-4-methyl-7-hydroxycoumarin

J. Sérgio Seixas de Melo*,† and António L. Maçanita*,‡

†Coimbra Chemistry Centre, Department of Chemistry, University of Coimbra, Rua Larga, 3004-535 Coimbra, Portugal

‡Centro de Química Estrutural, Instituto Superior Técnico, University of Lisbon, Av. Rovisco Pais s/n, 1049-001 Lisboa, Portugal

Supporting Information

ABSTRACT: The prototropic reactions of the first excited singlet state of 3-chloro-4-methylumbelliferone (3Cl4MU), in dioxane:water mixtures (Dx:H_2O), were revisited using ps-time-resolved fluorescence techniques. The data response to the dielectric constant of the mixtures revealed the presence of an additional fourth kinetic species, kinetically coupled to the neutral (N*), the tautomeric (T*), and anionic (A^-*) forms of 3Cl4MU, which is assigned to the elusive geminate (A^-*···H^+) ion pair. From the data analysis, all rate constants of the prototropic and diffusion processes involved were separately evaluated. The results showed that, whenever the geminate ionic pair is not kinetically detected, the evaluated values for deprotonation and protonation rate constants can substantially deviate from the real ones, depending on the efficiencies of pair recombination and dissociation. Finally, the results provide convincing kinetic evidence for the Eigen-Weller mechanism (intermediacy of the geminate ionic pair) in a quasi-aqueous medium, which to our knowledge had not yet been given.

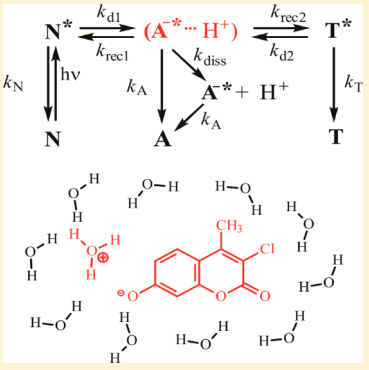

1. INTRODUCTION

In the 1960s, Manfred Eigen proposed the intermediacy of an ion pair in proton transfer (PT) reactions.[1] Within this model, PT involves three reversible processes: (1) diffusion-controlled formation and dissociation of the acid−base pair (encounter complex), (2) PT yielding the ions pair, which can revert to the encounter complex, and (3) diffusion-controlled separation of the ion pair to yield the free base and hydrated proton. For PT to water, in aqueous solution, the two first diffusional processes (1) can be ignored, thus reducing the system to processes (2) and (3), Scheme 1.

Scheme 1. Processes (2) and (3)

$$AH \rightleftharpoons A^- \cdots H^+ \rightleftharpoons A^- + H^+$$

Because the Eigen ion pair (A^-···H^+) and the free base (A^-) are spectroscopically undistinguishable, they can only be identified kinetically, either by separating the PT from proton diffusion steps as in Scheme 1[2−10] or by profiting from the nonexponential kinetics of diffusion-controlled recombination of the geminate A^- and H^+ (the $t^{-3/2}$ asymptotic decay).[11−18] However, to the best of our knowledge, such a separation has not yet been achieved in water.[12,14,15,18]

7-Hydroxycoumarins, or umbelliferones, often present more than two species in the excited state at pH values where only the neutral form N exists in the ground state.[19−22] Specifically, in dioxane:water mixtures (pH 5.5), the neutral acid N*, the anionic base A^-*, and the tautomeric T* forms of 7-hydroxycoumarin can be observed, depending on the dielectric constant of the mixture (Scheme 2).[20,21]

Scheme 2. Neutral Acid N*, Anionic Base A^-*, and Tautomeric T* Forms of 4-methyl-7-hydroxycoumarin

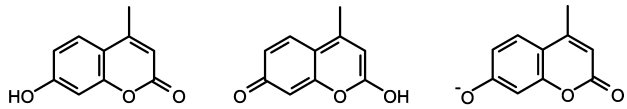

Previously, excited-state proton transfer kinetics of 3Cl4MU and 4-methylumbeliferone (4MU) in water and dioxane:water (Dx:H_2O) mixtures have been discussed, assuming direct formation of T* from N*.[19,20] Indeed, at low water content, (1) the fluorescence spectra showed only the emission bands of N* and T*, with an isoemissive wavelength, and (2) the fluorescence decays were well-fitted with sums of two exponential terms at all wavelengths along the fluorescence spectrum, strongly indicating the presence of just these two species. Only at higher concentrations of water has the emission of A^-* been detected, with the decays becoming triple exponentials. The apparently direct formation of T* from N* (bypassing the formation of A^-*) in low dielectric constant solvents has been interpreted on the basis of the so-called "push−pull" mechanism, which assumes synchronized depro-

Special Issue: Photoinduced Proton Transfer in Chemistry and Biology Symposium

Received: August 30, 2014
Revised: October 13, 2014
Published: October 17, 2014

   dx.doi.org/10.1021/jp508782h | J. Phys. Chem. B 2015, 119, 2604−2610

tonation and protonation of the hydroxyl and carbonyl groups of N*, respectively, through a bridge of hydrogen-bonded water molecules.[23,24] However, it has always been puzzling that such water molecular wires are efficiently formed in binary water:solvent mixtures with very low water content. In this work, with 3Cl4MU, we have profited from the effect of the dielectric constant (ε_0) on the dissociation rate constant of the ion pair, to kinetically distinguish/discriminate the anionic form (A^-*) from the ion pair (A^-*···H^+) and, thus, to evaluate the true values of the four rate constants of the two, PT and diffusion, processes.

2. EXPERIMENTAL SECTION

2.1. Materials. 3-Chloro-7-hydroxy-4-methylcoumarin (3Cl4MU) was purchased from Aldrich and its methoxylated parent compound, 3-chloro-7-methoxy-4-methylcoumarin (ClMMC), was synthesized and purified as described elsewhere.[25] Water was twice distilled and passed through a Millipore (Millipore Milli-Q grade) apparatus. Dioxane (Merck, Uvasol or Aldrich spectroscopic grade) was used without further purification or purified with procedures described elsewhere.[25] The concentration of the solutions was 1×10^{-5} M, and the pH was 5.5 (adjusted with stock solutions of $HClO_4$) or 12.5 (adjusted with stock solutions of NaOH). The solutions were deoxygenated either by N_2 or Ar bubbling.

2.2. Methods. The pH of solutions was measured with a Crison micropH 2000 pH meter. Absorption and fluorescence spectra were run with a Shimadzu UV-2100 spectrophotometer and a Horiba-Jobin-Ivon SPEX Fluoromax 3.22 spectrofluorimeter, respectively. Fluorescence emission and excitation spectra were corrected for the wavelength response of the system. The fluorescence quantum yields were measured using as standards: 3-chloro-7-methoxy-4-methylcoumarin (Φ_F = 0.12 in cyclohexane[25]) and α-terthienyl (Φ_F = 0.054 in ethanol[26]).

Fluorescence decays were obtained using the time-correlated single-photon-counting technique with different apparatus (with picosecond and nanosecond time resolution) as described elsewhere.[27−29] The decays were measured at three emission wavelengths, with different time/channel ratios, ranging from 0.81 to 24.4 ps/channel, due to the large range of decay times found (from 50 ps to 5 ns). The analysis was carried out by global fitting of sums of three and four exponential functions, convoluted with the impulse function, using the modulating functions method.[30,31] The impulse function of the picosecond equipment had a fwhm of 18−21 ps in the timescale of 0.81 ps/channel.[27,28]

3. RESULTS AND DISCUSSION

3.1. Absorption, Fluorescence Emission, and Fluorescence Excitation Spectra of 3Cl4MU. The absorption spectra of 3Cl4MU in dioxane:water (pH = 5.5) mixtures (Figure 1a) are identical to the absorption spectra of the methoxylated parent compound (3-chloro-7-methoxy-4-methylcoumarin; ClMMC) in the same mixtures,[25,32] showing that the neutral form (N) is the unique absorbing species.

The fluorescence spectra of 3Cl4MU show three emission bands of N*, T*, and A^-* (Figure 1b). In pure dioxane, only the emission from the excited neutral form (N*) is observed, with λ_{max}= 393 nm.[19] Addition of water first induces the appearance of an emission shoulder with λ_{max} = 510 nm, assigned to the tautomeric form (T*). For water mole fractions (x_w) above 0.50, the excited anion (A^-*) emission, at λ_{max} =

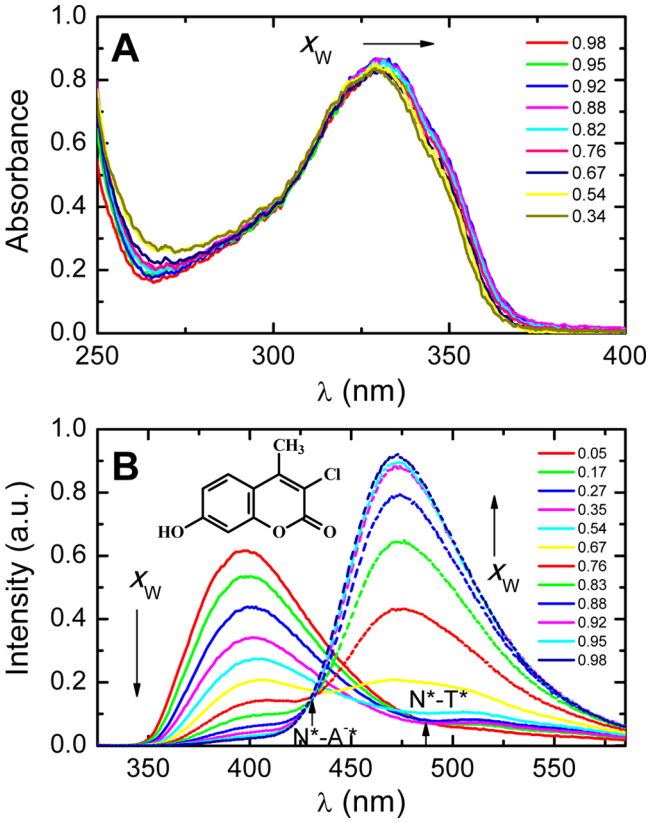

Figure 1. (A) Absorption and (B) fluorescence emission spectra (λ_{exc} = 296 nm) of 3Cl4MU in dioxane:water mixtures with different mole fractions of water (x_w) at T = 20 °C; the pH of the water in these mixtures, before addition of dioxane, was equal to 5.5. Two clear isoemissive points (N*-A^-* and N*-T*) are observed.

473 nm, appears (light-blue spectrum in Figure 1b), becoming the dominant emission at the highest x_w values. For x_w = 0.05−0.35, the spectra essentially displays the emission of N* and T*, whereas for x_w = 0.67−0.98, the emissions are essentially those of N* and A^-*. In both cases, clear isoemissive points are observed at 489 and 430 nm, respectively.

The excitation spectra, collected at any emission wavelength along the observed emissions, are identical to the absorption spectra of N in the respective solvent mixture, confirming that A^-* and T* are formed in the excited state at expenses of N*. In the same dioxane:water mixtures but in alkaline media (pH = 12.5), the absorption spectra correspond to that of the anionic form (A^-).

Fluorescence quantum yields and lifetimes of the neutral form of 3Cl4MU in dioxane:water mixtures were measured with the parent compound 3-chloro-4-methyl-7-methoxycoumarin (ClMMC), which cannot deprotonate. Those of the anionic form were measured with 3Cl4MU at pH 12.5 (the only form in the ground state at this pH value). The values of ϕ_0 and τ_0, as well as those of the radiative rate constants (k_F), are presented in Table 1, which collects additional steady-state fluorescence data of N* and A^-*.

3.2. Fluorescence Decays of 3Cl4MU in Dioxane:Water Mixtures. The fluorescence decays of 3Cl4MU in dioxane:water (pH = 5.5) mixtures, resulting from excitation at 360 nm (Figure 2), were collected at 380 nm (emission of N*), 480 nm (emission of A^-* with contributions of N* and T*) and 550 nm (emission due to both T* and A^-*). For dioxane:water mixtures with low water content (for

dx.doi.org/10.1021/jp508782h | J. Phys. Chem. B 2015, 119, 2604−2610

Table 1. Fluorescence Quantum Yields (ϕ_0), Lifetimes from Single-Exponential Decays (τ_0), and Radiative Rate Constants (k_F) of the Neutral and Anionic Forms of 3Cl4MU in Dioxane:Water Mixtures as a Function of the Mole Fraction of Water, x_w

x_w	ϕ_0^{N*a}	τ_0^{N*}/ns^a	$k_F^{N*}/10^9$ s^{-1}	ϕ_0^{A-*b}	τ_0^{A-*}/ns^b	$k_F^{A-*}/10^9$ s^{-1}
0.35	0.66	3.10	0.21	–	5.21	–
0.54	0.68	3.30	0.21	0.74	5.30	0.14
0.67	0.76	3.47	0.22	–	5.40	–
0.76	0.78	3.58	0.22	0.73	5.09	0.14
0.83	0.84	3.70	0.23	–	5.34	–
0.88	0.83	3.80	0.22	0.76	5.32	0.14
0.92	0.84	3.90	0.22	–	5.32	–
0.95	0.83	3.90	0.21	–	5.42	–
0.98	0.82	3.94	0.21	0.80	5.31	0.15

^{a}Measured with the parent compound 3-chloro-4-methyl-7-methoxycoumarin.[25] ^{b}Measured at pH 12.5.

x_w < 0.5), the decays required sums of three exponential terms for appropriate fitting (Figure 2a), while for x_w > 0.5, four exponentials were required (Figure 2b). This indicates the presence of one additional species, not discernible in the emission spectra, besides N* and T* for x_w < 0.5, and N*, T*, and A^-* for x_w > 0.5. The decay times and pre-exponential coefficients resultant from the fittings are plotted in Figure 3, as well as the lifetime of A^-* measured in the same mixtures at pH 12.5.

For x_w < 0.5 (triple exponential decays), the two intermediate decay times (τ_3 and τ_2) are dominant at all wavelengths (Figures 3, panels b–d) and remain approximately constant with values of ca. 0.6 and 1.4 ns, respectively (Figure 3a), while their pre-exponential coefficients at 380 nm (A_{13} and A_{12}, Figure 3b) abruptly change in reverse order in this x_w range. The shortest decay time (τ_4) decreases slightly from ca. 200 to 130 ps, appearing as rise time at 480 nm and decay time at 550 nm. The puzzling observation within this x_w range is the absence of the typical lifetime of the free base A^-* ($\tau_{A^*} \approx 5$ ns at pH 12.5, open triangles in Figure 3a) in the decays, in spite of clear occurrence of deprotonation of N* (strong fluorescence quenching of N*). There are only two possible explanations for this observation: (1) either the deprotonation of N* directly yields T* (push–pull mechanism) or (2) it first yields A^-*···H^+, but then the recombination efficiency of A^-*···H^+, yielding T* (and/or N*), must be close to 100%, leading to the nonobservation of the free A^-* emission. The first possibility involves two excited species (N* and T*), which should give rise to double exponential decays, while the second, involving three species, should lead to triple-exponential decays. The experimental observation of triple-exponential decays for x_w < 0.5 strongly supports the second possibility that deprotonation of N yields the ion pair A^-*···H^+, appearing as a kinetically distinguishable species in the reactions network. The implicit high recombination efficiency of this last hypothesis can only result from a very low value of the dissociation rate constant of A^-*···H^+, incapable of competing with the respective recombination rate constants.

Above x_w = 0.5, the fourth decay component, with decay times (τ_1) close to the lifetime of A^-* (τ_{A^-}*) at pH 12.5, appears. For x_w = 0.54 and 0.67, the τ_1 values are slightly shorter than τ_{A^-}* (4.2 and 4.7 ns vs 5.3 ns), indicating that for these mixtures A^-* is not entirely "free", probably due to geminate recombination with H^+ located at the second or third

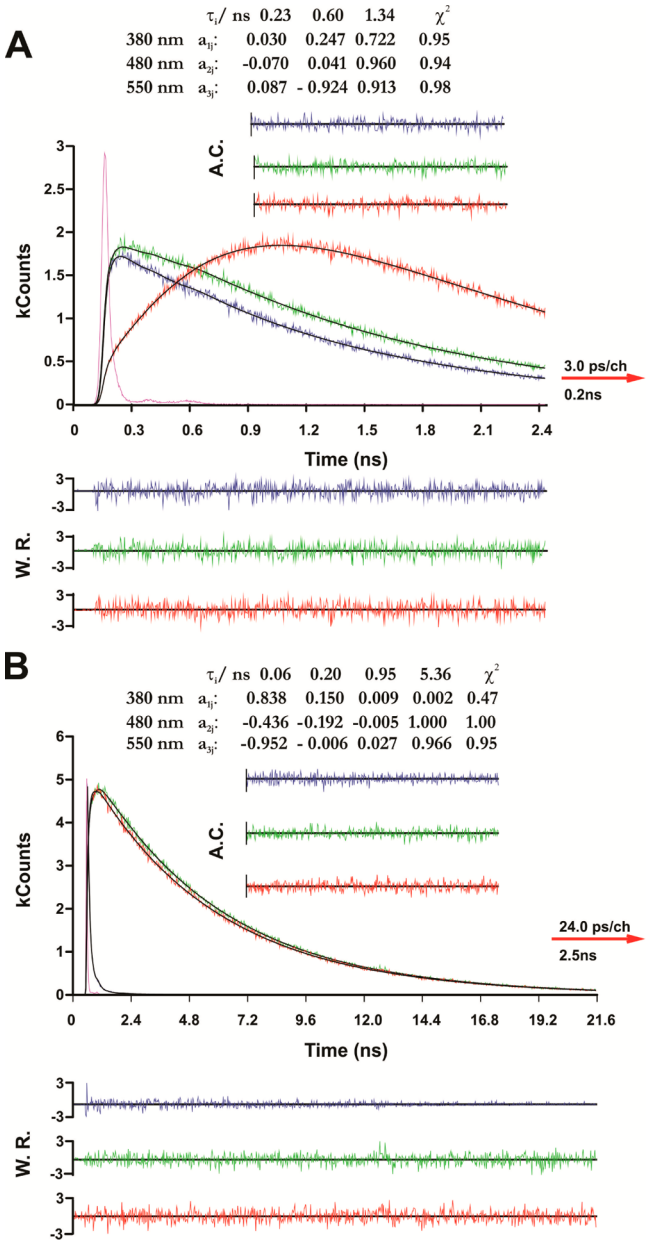

Figure 2. Global analysis of fluorescence decays of 3Cl4MU in dioxane:water mixtures, excited at λ_{exc}= 360 nm, and measured at 380, 480, and 550 nm at T = 293 K: (A) x_w = 0.15 (pH = 5.5), with 3.05 ps/channel; (B) x_w = 0.83 with 24.3 ps/channel. The pulse profile (pink line), weighted residues (W.R.), chi-squared values (χ^2), and autocorrelation functions (A.C.) are also shown.

solvation shell. Above x_w = 0.5, the remaining decay times (τ_2, τ_3, and τ_4) abruptly decrease with the increase of x_w. This decrease indicates a sharp increase of one or more rate constants above x_w = 0.5, namely those associated with the formation of the free base. For the highest x_w value (x_w = 0.98), the shortest decay time (τ_4) decreases to 44 ps and the pre-exponential coefficients of τ_2 and τ_3 (A_{i2} and A_{i3}) tend to zero (i.e., the decays become quasi-double exponential in water).

In summary, the data indicates the presence of a fourth kinetic species besides N*, T*, and A^-*, likely the Eigen ion pair, in the reactions network shown in Scheme 3. This possibility will be analyzed in detail in the next two sections.

dx.doi.org/10.1021/jp508782h | J. Phys. Chem. B 2015, 119, 2604–2610

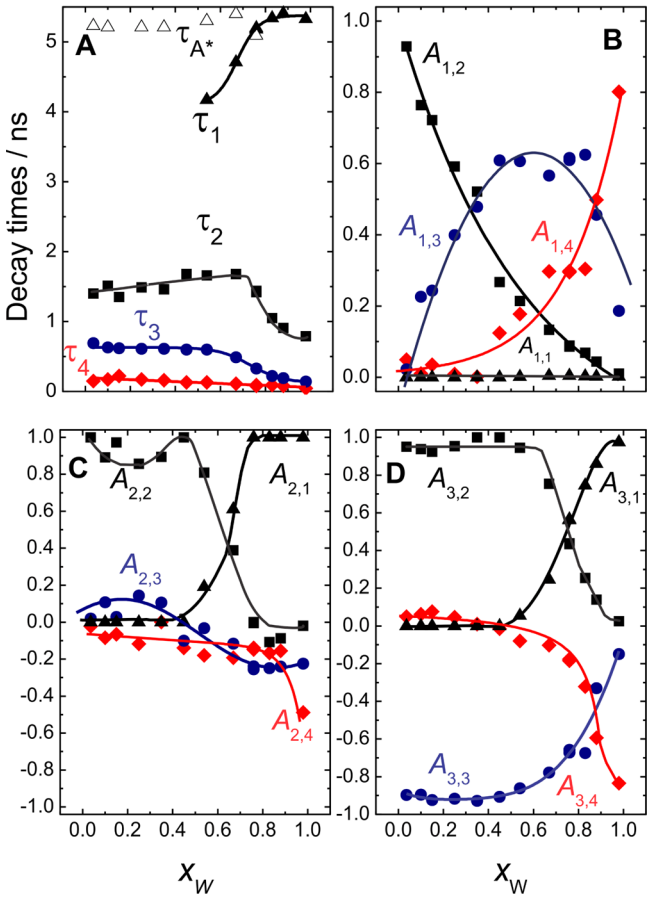

Figure 3. Plots of the (A) decay times τ_i, and pre-exponential coefficients at (B) λ_{em} = 380 nm, (C) λ_{em} = 480 nm, and (D) λ_{em} = 550 nm, measured for 3Cl4MU in Dx:H_2O (pH = 5.5) mixtures at 20 °C, with λ_{exc}= 360 nm and 3 ps/channel. The △ in (A) are the lifetimes of A^-* measured in Dx:H_2O with water at pH 12.5. The lines are just meant to be guides to the eye.

Scheme 3. Reactions Network

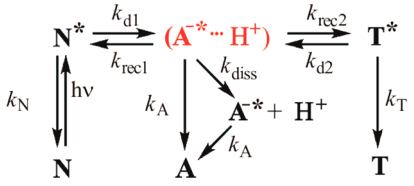

3.3. Data Analysis. Scheme 3 leads to a system of four linear differential equations (eq 1), which predicts sums of four exponential terms for the excited state concentrations of X_i = N*, (A^-*···H^+), T*, and A* (eq 2).[4]

$$\frac{d}{dt}\begin{bmatrix} N^* \\ A^-{}^*\cdots H^+ \\ T^* \\ A^* \end{bmatrix} = \begin{bmatrix} -X & k_{rec1} & 0 & 0 \\ k_{d1} & -Y & k_{d2} & 0 \\ 0 & k_{rec1} & -Z & 0 \\ 0 & k_{diss} & 0 & -W \end{bmatrix} \cdot \begin{bmatrix} N^* \\ A^-{}^*\cdots H^+ \\ T^* \\ A^- \end{bmatrix} \quad (1)$$

$$[X_i] = a_{i,1}e^{-\lambda_1 t} + a_{i,2}e^{-\lambda_1 t} + a_{i,3}e^{-\lambda_1 t} + a_{i,4}e^{-\lambda_1 t} \quad (2)$$

In eqs 1 and 2, $X = k_N + k_{d1}$, $Y = k_A + k_{rec1} + k_{rec2} + k_{diss}$, $Z = k_T + k_{d2}$, $W = k_A$, the four reciprocal decay times ($\lambda_i = 1/\tau_i$) are the roots of the characteristic equation (eq 3), and the pre-exponential coefficients $a_{i,j}$ are linear combinations of the eigenvectors of the rate constants matrix **k** that satisfy the initial conditions: $\Sigma_{j=1}^{4} a_{1,j} = 1$; $\Sigma_{j=1}^{4} a_{2,j} = 0$, $\Sigma_{j=1}^{4} a_{3,j} = 0$, $\Sigma_{j=1}^{4} a_{4,j} = 0$.

One of the roots of the characteristic equation is $\lambda_1 = k_A$ (protonation of A* at pH 5.5 is negligible), and the other three are the roots of the remaining third degree equation.

$$\begin{vmatrix} \lambda - X & k_{rec1} & 0 & 0 \\ k_{d1} & \lambda - Y & k_{d2} & 0 \\ 0 & k_{rec1} & \lambda - Z & 0 \\ 0 & k_{diss} & 0 & \lambda - W \end{vmatrix} = 0 \quad (3)$$

The rate constants matrix **k** can be expressed as a function of the reciprocal decay times ($\lambda_j = 1/\tau_j$) matrix **λ**, and the pre-exponential coefficients ($a_{i,j}$) matrix **a**, as[20,33]

$$\mathbf{k} = \mathbf{a}\boldsymbol{\lambda}\mathbf{a}^{-1} \quad (4)$$

The evaluation of **k** from the fluorescence data is detailed in the Supporting Information. Briefly, the analysis consisted in converting the **a** matrix (concentrations) into the experimental **A** matrix (fluorescence intensities), and then calculating the **λ** and **A** matrixes with the [vec,val] = eig(k) Matlab function,[20] from an initial guess of the **k** matrix, and finally optimizing **k** with the Matlab *fminsearch* subroutine,[20] by minimizing the residuals of $\boldsymbol{\lambda}_{exp}-\boldsymbol{\lambda}_{calc}$ and $\mathbf{A}_{exp}-\mathbf{A}_{calc}$. The results are shown in Table 2 and plotted in Figure 4.

3.4. Dissociation of the Eigen Pair. The dissociation rate constant of the geminate pair (• in Figure 4a) is practically equal to zero for x_w < 0.5, meaning that in this range of x_w the photogenerated proton does not escape from the first solvation shell of A^-*, and the typical lifetime of the free base A^-* ($\tau_{A^*} \approx$ 5 ns, △ in Figure 3a) should not be observed.

Figure 4a also shows values of k_{diss} calculated with the Debye-Smoluchowski eq 5[41] (• in Figure 4a), assuming the Eigen proton ($H_9O_4^+$) structure for calculation of van der Waals radii ($R = R_A + R_{proton}$) and diffusion coefficients ($D = D_A + D_{proton}$).

$$k_{diss}(calc) = \frac{3D}{R^2} \times \frac{\Delta U_{el}/RT}{1 - e^{-\Delta U_{el}/RT}} \quad (5)$$

with $\Delta U_{el} = e^2 N_A/4\pi\varepsilon\varepsilon_0 R$.

Taking into account the arbitrary choice of the Eigen ion structure and the inadequacy of the Stokes−Einstein equation used here for evaluation of the proton diffusion coefficient (D_{proton}), qualitatively, the agreement between experimental and calculated values of k_{diss} shown in Figure 4a is quite good. The important point, however, is that below x_w = 0.5 (ε_0 < 10), the electrostatic potential energy ($-\Delta U_{el}$) is so large that the (calculated) values of k_{diss} are less than 10^8 s^{-1}, while the sum of the recombination rate constants $k_{rec1} + k_{rec2}$ is larger than 2 × 10^9 s^{-1} (Figure 4a). This implies recombination efficiencies larger than 95% (i.e., less than 5% of the ion pair is able to dissociate), explaining why the free base is not observed for x_w < 0.5.

With the increase of x_w and the concomitant increase of ε_0, the dissociation rate constant, k_{diss}, sharply increases up to values close to diffusion-controlled dissociation in water, allowing the formation (and observation) of the free base for $x_w \geq 0.5$. The sharp increase of k_{diss} together with that of k_{d1} for $x_w \geq 0.5$ are the cause for the abrupt decrease of τ_3 and τ_4 in

dx.doi.org/10.1021/jp508782h | J. Phys. Chem. B 2015, 119, 2604−2610

Table 2. Rate Constants of the Prototropic Reactions of 3Cl4MU in Dioxane:Water Mixtures, at pH 5.5 and T = 20 °C[a]

x_w	η[b] (cP)	ε_0[c]	k_{d1} (ns^{-1})	k_{d2} (ns^{-1})	k_{rec1} (ns^{-1})	k_{rec2} (ns^{-1})	k_{diss} (ns^{-1})	k_{diss}(calc)[d] (ns^{-1})
0.03_5	1.32	2.4	0.2	2.9	1.5	0.5	0	0
0.10	1.34	2.9	0.2	2.6	2.1	1.8	0	0
0.15	1.36	3.2	0.3	1.9	2.1	1.1	0	0
0.25	1.42	4.3	0.4	2.6	1.4	2.2	0	0
0.35	1.54	6.1	0.3	1.6	1.6	3.4	0	0
0.45	1.73	8.2	1.5	0.8	3.3	3.2	0.05	0.01
0.54	1.94	11	1.9	0.6	3.5	2.8	0.1	0.04
0.67	2.21	18	3.3	0.6	3.4	2.2	0.9	0.34
0.76	2.27	28	4.6	0.9	3.1	3.2	1.6	1.33
0.83	2.17	36	5.9	1.6	2.1	3.6	2.3	2.38
0.88	1.98	45	8.2	1.6	2.1	3.1	3.0	3.68
0.92	1.75	55	10.5	0.5	1.3	0.2	3.7	5.26
0.95	1.52	63	11.3	0.3	1.0	0.1	5.0	7.00
0.98	1.23	72	19.1	1.4	1.9	0.7	7.3	9.69
1.00	1.00	78	–	–	–	–	–	12.62

[a]Viscosities (η) and dielectric constant (ε_0) of the mixtures are also shown. [b]Values interpolated from data in ref 34. [c]Values interpolated from data in ref 35. [d]Calculated with equation 5.

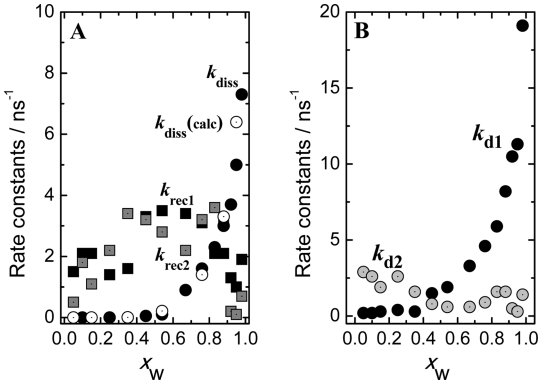

Figure 4. Plots of rate constants of (A) geminate pair recombination [k_{rec1} (black ■) and k_{rec2} (gray ■)] and dissociation [k_{diss} (black •) and k_{diss}(calc) (○)] and (B) deprotonation of the neutral form [k_{d1} (•)] and tautomer [k_{d1} (gray •)] of 3Cl4MU in Dx:H_2O (pH = 5.5) mixtures vs the mole fraction of water x_w. Values are given in Table 2.

this x_w region (Figure 3a). It is important to note that a similar effect of ε_0 on the dissociation of charged species was pointed out by Albert Weller when discussing the relative stability of the exciplex, ion pair, and solvent-separated ion-pair in photo-induced charge/electron transfer reactions.[36,37] Exciplexes are generally observed only for ε_0 < ca. 10, while for higher ε_0 values, the solvent-separated ion-pair (radical ions) is the main reaction product. A last piece of information, in support of the foregoing discussion, is the fact that we observed the free base lifetime of 3Cl4MU in methanol:water mixtures (ε_0 > 37) for all compositions.

In summary, the distinction between the spectroscopically identical A^{-}* and (A^{-}*···H^+) species can be accomplished by preventing the formation of A^{-}* at low values of ε_0 (< ca. 10), and then increasing ε_0 until the fraction of (A^{-}*···H^+) becomes undetectable due to fast dissociation.

3.5. Apparent and Real Values of the PT Rate Constants. Fluorescence decays of 3Cl4MU in water were previously measured by us as a function of the pH, using different apparatus.[19] The decays could be barely fitted with sums of two exponentials terms, which were assigned to the two spectroscopically observed N* and A^{-}* forms. The kinetic analysis of results with the Birks' type mechanism[19,33,38,39] (one ground state species giving rise to two excited species in equilibria) provided a value of k_p = 2.2 × 10^{10} M^{-1} s^{-1} for the protonation rate constant k_p in water.[19] Although this value has been considered to be in the range of diffusion-controlled protonation in water, it is substantially lower than the theoretical value of k_{diff} for the 3Cl4MU···H^+ pair (k_{diff} = 8 × 10^{10} M^{-1} s^{-1}), when the experimental value of the diffusion coefficient of the proton in water (ca. 9 × 10^{-5} cm^2 s^{-1}) and the calculated radius of the Eigen ion (2.42 Å) are used for the calculation with the Debye-Smoluchovski equation.[40,41] This would imply that some of the encounters between A^{-}* and H^+ do not lead to protonation [i.e., that the efficiency of protonation, γ_{rec} = $k_{rec}/(k_{rec} + k_{diss})$, is lower than unity]. This possibility can be checked with the dioxane:water mixture closest to pure water, x_w = 0.98, for which the values of k_{rec1} +

Table 3. Simulated Decays of N*, (A^{-}*···H^+), T* and A^{-}* with Two Sets of Rate Constants: (1) Those Obtained for x_w = 0.98 and (2) the Same Rate Constants Except for k_{rec1} and k_{rec2}, Both Set at 0.1 ns^{-1}

	rate constants set 1				rate constants set 2			
pre-exponential	τ_1 (ns)	τ_2 (ns)	τ_3 (ns)	τ_4 (ns)	τ_1(ns)	τ_2 (ns)	τ_3 (ns)	τ_4 (ns)
coefficients	5.32	0.57	0.14	0.04	5.32	0.53	0.13	0.05
A_{1j} (N*)	**0.00**	**0.00**	**0.18**	**0.82**	**0.00**	**0.00**	**0.01**	**0.99**
A_{2j}(A^{-}*···H^+)	0.00	0.03	1.23	−1.26	0.00	0.00	1.55	−1.55
A_{3j} (T*)	**0.00**	**0.11**	**−0.16**	**0.04**	**0.00**	**0.02**	**−0.03**	**0.01**
A_{4j} (A^{-}*)	0.96	−0.12	−1.25	0.41	0.98	−0.02	−1.53	0.58
A_{2j} (A^{-}*···H^+) + A_{4j} (A^{-}*)	**0.96**	**−0.09**	**−0.02**	**−0.84**	**0.98**	**−0.02**	**0.01**	**−0.98**

dx.doi.org/10.1021/jp508782h | J. Phys. Chem. B 2015, 119, 2604−2610

k_{rec2} and k_{diss} are ca. 2.6 and 7.3 ns^{-1}, respectively. From these values, the efficiency of proton recombination of $A^{-}*\cdots H^{+}$ to yield N* is $\gamma_{rec} \approx 0.26$. If this value, $\gamma_{rec} = 0.26$, is assumed to be valid for pure water, from $k_{diff} = k_p/\gamma_{rec}$, we obtain a value of $k_{diff} = 8.4 \times 10^{10}$ M^{-1} s^{-1}, very close to the calculated one (8×10^{10} M^{-1} s^{-1}), and much larger than the (apparent) rate constant for protonation, $k_p = 2.2 \times 10^{10}$ M^{-1} s^{-1}.

Another important result from the Eigen pair detection concerns the proton transfer rate constant. In this work, we observed that the value of k_{d1} increases up to 1.9×10^{10} s^{-1} for $x_w = 0.98$, which is larger than the value previously obtained from Birks' analysis in water ($k_d = 1.5 \times 10^{10}$ s^{-1}).[19] Again, assuming that the $x_w = 0.98$ data can be extrapolated to water, the efficiency of pair dissociation, $\gamma_{diss} = k_{diss}/(k_{rec1}+k_{diss})$, is $\gamma_{diss} = 0.74$, and the (true) value of the deprotonation rate constant in water would be $k_{d1} = k_d/\gamma_{diss} = 2.0 \times 10^{10}$ s^{-1}, a value identical to the extrapolated k_{d1}.

Summarizing, the distinction between $A^{-}*$ and $(A^{-}*\cdots H^{+})$ permits, in principle, the evaluation of true values of PT rate constant, cleaned from diffusion contributions. These values may substantially differ from those of the respective apparent PT rate constants and be useful for testing current modeling of proton transfer.[42−44]

3.6. Why is it Difficult to Detect the Ion Pair in Water?

Table 3 shows the four decay times and pre-exponential coefficients of the four species [N*, $(A^{-}*\cdots H^{+})$, T*, and $A^{-}*$] calculated with two sets of rate constants: (i) the rate constants obtained for $x_w = 0.98$ and (ii) the same values of rate constants except for k_{rec1} and k_{rec2}, which were set equal to an arbitrary value of 0.1 ns^{-1} plausible for water on the basis of the tendency of k_{rec1} and k_{rec2} to decrease with increasing x_w (Figure 4a). The spectral overlaps were not included in the calculated values of the pre-exponential coefficients for clarity. Rows 1, 3, and 5 show the experimentally detectable pre-exponential coefficients of N*, T*, and the sum of the pair A_2 $(A^{-}*\cdots H^{+})$ and free base A_4 ($A^{-}*$) that would be measured at 380, 480, and 550 nm in the absence of spectral overlap.

The first aspect to remember is that the geminate ionic pair and the free base display the same fluorescence spectrum, lifetime, and quantum yield. Therefore, the observed decay of $(A^{-}*\cdots H^{+}) + A^{-}*$ is the sum of the individual decays at any emission wavelength (last row of Table 3). Second, because $A^{-}*$ is generated from $(A^{-}*\cdots H^{+})$, the pre-exponential coefficients of the three shorter decay times have opposite signs in the decays of $A^{-}*$ and $(A^{-}*\cdots H^{+})$. When both k_{rec1} and $k_{rec2} \ll k_{diss}$, the opposite signs lead to partial (rate constants set 1) or total (rate constants set 2) cancelation of pre-exponential coefficients of the two intermediate decay times (τ_2 and τ_3). Thus, for total cancelation, the fluorescence decays of all species (rows in bold for rate constants set 2) would be experimentally nondistinguishable from double-exponential decays, which essentially report the kinetics of N* and $A^{-}*$.

In summary, the difficulty to experimentally detect the ion pair in water is ascribed to the effect of the high dielectric constant of water on the recombination and dissociation of the ion pair. At high values of the dielectric constant, the dissociation rate constant reaches quasi-diffusion-controlled dissociation values due to the weakening of the electrostatic attraction of the pair, while the recombination rate constants reach minimum values due to preferential pair stabilization relative to the neutral N* and T* forms. Under these conditions of $k_{diss} \gg k_{rec}$, the "witness" of the ionic pair presence (the additional exponential term) disappears due to the aforementioned cancelation of its pre-exponential coefficient.

CONCLUSIONS

The foregoing results and discussion provide a number of contributions to the understanding of proton transfer reactions: (1) the clarification of the prototropic reaction mechanism of 3Cl4MU (and probably of most 7-hydroxycoumarins) (i.e., the intermediacy of the geminate ionic pair in the tautomerization and formation of the free base), rather than a "push-pull mechanism"; (2) the demonstration that whenever the geminate ionic pair is not detected in acid−base reactions, the evaluated values for deprotonation and protonation rate constants can substantially deviate from the true values, depending on the efficiencies of pair recombination and dissociation, and finally, (3) the experimental proof for the Eigen-Weller mechanism in a quasi-aqueous medium, which to our knowledge has not yet been given. Additionally, a comprehensive analysis of the variables that control the detection of the geminate pair, such as the solvent dielectric constant, is also given. These contributions may be particularly relevant for the analysis of naturally occurring proton transfer reactions in mixed aqueous media, as in biological systems.

ASSOCIATED CONTENT

Supporting Information

Data analysis and Accuracy of results. This material is available free of charge via the Internet at http://pubs.acs.org.

AUTHOR INFORMATION

Corresponding Authors

*E-mail: sseixas@ci.uc.pt.

*E-mail: macanita@ist.utl.pt.

Notes

The authors declare no competing financial interest.

ACKNOWLEDGMENTS

This work was supported by the Portuguese Science Foundation (FCT), Portugal, Projects PTDC/QUI-QUI/116249/2009 and PEst-OE/QUI/UI0100/2011. The Coimbra Chemistry Centre is supported by FCT through the project PEst-OE/QUI/UI0313/2014.

REFERENCES

(1) Eigen, M. Proton Transfer, Acid-Base Catalysis, and Enzymatic Hydrolysis. Part I: Elementary Processes. *Angew. Chem., Int. Ed.* **1964**, *3* (1), 1−19.

(2) Freitas, A. A.; Quina, F. H.; Maçanita, A. L., Femtosecond and Temperature-Dependent Picosecond Dynamics of Ultrafast Excited State Proton Transfer in Water-Dioxane Mixtures *J. Phys. Chem. B* **2014**, (Special issue) DOI: 10.1021/jp504189m.

(3) Freitas, A. A.; Quina, F. H.; Maçanita, A. L. Picosecond Dynamics of Proton Transfer of a 7-Hydroxyflavylium Salt in Aqueous-Organic Solvent Mixtures. *J. Phys. Chem. A* **2011**, *115* (40), 10988−10995.

(4) Freitas, A. A.; Quina, F. H.; Fernandes, A. C.; Maçanita, A. L. Picosecond Dynamics of the Prototropic Reactions of 7-Hydroxyflavylium Photoacids Anchored at an Anionic Micellar Surface. *J. Phys. Chem. A* **2010**, *114* (12), 4188−4196.

(5) Paulo, L.; Freitas, A. A.; da Silva, P. F.; Shimizu, K.; Quina, F. H.; Maçanita, A. L. Novel Ground- And Excited-State Prototropic Reactivity of a Hydroxycarboxyflavylium Salt. *J. Phys. Chem. A* **2006**, *110* (6), 2089−2096.

(6) Freitas, A. A.; Paulo, L.; Maçanita, A. L.; Quina, F. H. Acid-Base Equilibria and Dynamics in Sodium Dodecyl Sulfate Micelles:

Geminate Recombination and Effect of Charge Stabilization. *Langmuir* **2006**, *22* (19), 7986−7993.
(7) Giestas, L.; Yihwa, C.; Lima, J. C.; Vautier-Giongo, C.; Lopes, A.; Maçanita, A. L.; Quina, F. H. The Dynamics of Ultrafast Excited State Proton Transfer in Anionic Micelles. *J. Phys. Chem. A* **2003**, *107* (18), 3263−3269.
(8) Rodrigues, R.; Vautier-Giongo, C.; Silva, P. F.; Fernandes, A. C.; Cruz, R.; Maçanita, A. L.; Quina, F. H. Geminate Proton Recombination at the Surface of SDS and CTAC Micelles Probed with a Micelle-Anchored Anthocyanin. *Langmuir* **2006**, *22* (3), 933−940.
(9) Brenlla, A.; Veiga Gutiérrez, M.; Ríos Rodríguez, M. C.; Rodríguez-Prieto, F.; Mosquera, M.; Pérez Lustres, J. L. Moderately Strong Photoacid Dissociates in Alcohols with High Transient Concentration of the Proton-Transfer Contact Pair. *J. Phys. Chem. Lett.* **2014**, *5* (6), 989−994.
(10) Brenlla, A.; Veiga, M.; Perez Lustres, J. L.; Rios Rodriguez, M. C.; Rodriguez-Prieto, F.; Mosquera, M. Photoinduced Proton and Charge Transfer in 2-(2′-Hydroxyphenyl)imidazo 4,5-b pyridine. *J. Phys. Chem. B* **2013**, *117* (3), 884−896.
(11) Pines, E.; Huppert, D. Observation of Geminate Recombination in Excited-State Proton-Transfer. *J. Chem. Phys.* **1986**, *84* (6), 3576−3577.
(12) Leiderman, P.; Genosar, L.; Huppert, D.; Shu, X.; Remington, S. J.; Solntsev, K. M.; Tolbert, L. M. Ultrafast Excited-State Dynamics in the Green Fluorescent Protein Variant S65T/H148D. 3. Short- and Long-Time Dynamics of the Excited-State Proton Transfer. *Biochemistry* **2007**, *46* (43), 12026−12036.
(13) Solntsev, K. M.; Clower, C. E.; Tolbert, L. M.; Huppert, D. 6-Hydroxyquinoline-N-Oxides: A new Class of "Super" Photoacids. *J. Am. Chem. Soc.* **2005**, *127* (23), 8534−8544.
(14) Tolbert, L. M.; Solntsev, K. M. Excited-State Proton Transfer: From Constrained Systems to "Super" Photoacids to Superfast Proton Transfer. *Acc. Chem. Res.* **2002**, *35* (1), 19−27.
(15) Solntsev, K. M.; Huppert, D.; Agmon, N.; Tolbert, L. M. Photochemistry of "Super" Photoacids. 2. Excited-State Proton Transfer in Methanol/Water Mixtures. *J. Phys. Chem. A* **2000**, *104* (19), 4658−4669.
(16) Solntsev, K. M.; Huppert, D.; Agmon, N. Photochemistry of "Super"-Photoacids. Solvent Effects. *J. Phys. Chem. A* **1999**, *103* (35), 6984−6997.
(17) Solntsev, K. M.; Huppert, D.; Tolbert, L. M.; Agmon, N. Solvatochromic Shifts of "Super" Photoacids. *J. Am. Chem. Soc.* **1998**, *120* (31), 7981−7982.
(18) Leiderman, P.; Huppert, D.; Agmon, N. Transition In The Temperature-Dependence of GFP Fluorescence: From Proton Wires to Proton Exit. *Biophys. J.* **2006**, *90* (3), 1009−1018.
(19) Seixas de Melo, J. S.; Cabral, C.; Lima, J. C.; Maçanita, A. L. Characterization of the Singlet and Triplet Excited States of 3-Chloro-4-methylumbelliferone. *J. Phys. Chem. A* **2011**, *115* (30), 8392−8398.
(20) Seixas de Melo, J.; Maçanita, A. L. Three Interconverting Excited Species: Experimental Study and Solution of the General Photokinetic Triangle By Time-Resolved Fluorescence. *Chem. Phys. Lett.* **1993**, *204* (5,6), 556.
(21) Cohen, B.; Huppert, D. Excited State Proton-Transfer Reactions of Coumarin 4 in Protic Solvents. *J. Phys. Chem. A* **2001**, *105* (30), 7157−7164.
(22) Simkovitch, R.; Kisin-Finfer, E.; Shomer, S.; Gepshtein, R.; Shabat, D.; Huppert, D. Ultrafast Excited-State Proton Transfer from Hydroxycoumarin-Dipicolinium Cyanine Dyes. *J. Photochem. Photobiol., A* **2013**, *254*, 45−53.
(23) Moriya, T. Excited-State Reactions of Coumarins in Aqueous-Solutions 0.1. The Phototautomerization of 7-Hydroxycoumarin and Its Derivative. *Bull. Chem. Soc. Jpn.* **1983**, *56* (1), 6−14.
(24) Moriya, T. Excited-State Reactions of Coumarins .7. The Solvent-Dependent Fluorescence of 7-Hydroxycoumarins. *Bull. Chem. Soc. Jpn.* **1988**, *61* (6), 1873−1886.
(25) Seixas de Melo, J.; Becker, R. S.; Elisei, F.; Maçanita, A. L. The Photophysical Behavior of 3-Chloro-7-Methoxy-4-Methylcoumarin Related to the Energy Separation of the Two Lowest-Lying Singlet Excited States. *J. Chem. Phys.* **1997**, *107* (16), 6062−6069.
(26) Becker, R. S.; Seixas de Melo, J.; Maçanita, A. L.; Elisei, F. Comprehensive Evaluation of the Absorption, Photophysical, Energy Transfer, Structural, and Theoretical Properties of Alpha-Oligothiophenes with One to Seven Rings. *J. Phys. Chem.* **1996**, *100* (48), 18683−18695.
(27) Rodrigues, R. F.; da Silva, P. F.; Shimizu, K.; Freitas, A. A.; Kovalenko, S. A.; Ernsting, N. P.; Quina, F. H.; Maçanita, A. L. Ultrafast Internal Conversion in a Model Anthocyanin-Polyphenol Complex: Implications for the Biological Role of Anthocyanins in Vegetative Tissues of Plants. *Chem.—Eur. J.* **2009**, *15* (6), 1397−1402.
(28) Pina, J.; Seixas de Melo, J.; Burrows, H. D.; Maçanita, A. L.; Galbrecht, F.; Bunnagel, T.; Scherf, U. Alternating Binaphthyl-Thiophene Copolymers: Synthesis, Spectroscopy, and Photophysics and Their Relevance to the Question of Energy Migration versus Conformational Relaxation. *Macromolecules* **2009**, *42* (5), 1710−1719.
(29) Seixas de Melo, J.; Fernandes, P. F. Spectroscopy and Photophysics of 4- and 7-Hydroxycoumarins and Their Thione Analogs. *J. Mol. Struct.* **2001**, *565*, 69−78.
(30) Striker, G. Effective Implementation of Modulation Functions. In *Deconvolution and Reconvolution Of Analytical Signals*, Bouchy, M., Ed. University Press: Nancy, France, 1982.
(31) Striker, G.; Subramaniam, V.; Seidel, C. A. M.; Volkmer, A. Photochromicity and Fluorescence Lifetimes of Green Fluorescent Protein. *J. Phys. Chem. B* **1999**, *103* (40), 8612−8617.
(32) Seixas de Melo, J. S.; Becker, R. S.; Maçanita, A. L. Photophysical Behavior of Coumarins as a Function of Substitution and Solvent: Experimental Evidence for the Existence of a Lowest Lying (1)(n,pi*) State. *J. Phys. Chem.* **1994**, *98* (24), 6054−6058.
(33) Birks, J. B. *Photophysics of Aromatic Molecules*; Wiley: London, 1970.
(34) Geddes, J. A. The Fluidity of Dioxane—Water Mixtures[1]. *J. Am. Chem. Soc.* **1933**, *55* (12), 4832−4837.
(35) Molotsky, T.; Huppert, D. Solvation Statics and Dynamics of Coumarin 153 In Dioxane-Water Solvent Mixtures. *J. Phys. Chem. A* **2003**, *107* (41), 8449−8457.
(36) Gordon, M.; Ware, W. R. *The Exciplex*; Academic Press: New York, 1975.
(37) Rini, M.; Pines, D.; Magnes, B. Z.; Pines, E.; Nibbering, E. T. J. Bimodal Proton Transfer in Acid-Base Reactions in Water. *J. Chem. Phys.* **2004**, *121* (19), 9593−9610.
(38) Laws, W. R.; Brand, L. Analysis of 2-State Excited-State Reactions: Fluorescence Decay of 2-Naphthol. *J. Phys. Chem.* **1979**, *83* (7), 795−802.
(39) Seixas de Melo, J. S.; Pina, J.; Dias, F. B.; Maçanita, A. L., Experimental Techniques for Excited State Characterisation. In *Applied Photochemistry*; Evans, R. C., Douglas, P., Burrows, H. D., Eds. Springer: Dordrecht, Holland, 2013; pp 533−585.
(40) Marx, D.; Chandra, A.; Tuckerman, M. E. Aqueous Basic Solutions: Hydroxide Solvation, Structural Diffusion, and Comparison to the Hydrated Proton. *Chem. Rev.* **2010**, *110* (4), 2174−2216.
(41) Rice, S. A.; Butler, P. R.; Pilling, M. J.; Baird, J. K. Solution of the Debye-Smoluchowski Equation for the Rate of Reaction of Ions in Dilute-Solution. *J. Chem. Phys.* **1979**, *70* (9), 4001−4007.
(42) Borgis, D.; Hynes, J. T. Curve Crossing Formulation for Proton Transfer Reactions in Solution. *J. Phys. Chem.* **1996**, *100* (4), 1118−1128.
(43) Kiefer, P. M.; Hynes, J. T. Nonlinear Free Energy Relations for Adiabatic Proton Transfer Reactions in a Polar Environment. I. Fixed Proton Donor-Acceptor Separation. *J. Phys. Chem. A* **2002**, *106* (9), 1834−1849.
(44) Kiefer, P. M.; Hynes, J. T. Nonlinear Free Energy Relations for Adiabatic Proton Transfer Reactions in a Polar Environment. II. Inclusion of the Hydrogen Bond Vibration. *J. Phys. Chem. A* **2002**, *106* (9), 1850−1861.